Open access e-Journal
Earth Science India eISSN: 0974 – 8350
v. 12 (IV), October, 2019, pp. 191-202
http://www.earthscienceindia.info/

Latitudinal Ionospheric Redistribution in Northern Hemisphere during Geomagnetic Storm

Mahesh Parwani[1], Roshni Atulkar[2], Rafi Ahmad[1], P.K. Sharma[3] and P.K. Purohit[2]
[1]Department of Physics, Barkatullah University, Bhopal (M.P.) India
[2]National Institute of Technical Teachers' Training & Research, Shyamla Hills, Bhopal, (M.P) India
[3]BUIT, Barkatullah University, Bhopal- 462026 (MP) India
Email: maheshkp.007.mp@gmail.com

ABSTRACT

The region around the Earth, where the magnetic field of the earth, dominates is known as Magnetosphere. The interaction between the solar wind and the magnetosphere gives rise to geomagnetic storms. These storms have deep terrestrial impacts. During the last some decades, our dependency on GPS navigation, communication and other applications has increased many folds, but the reliability of GPS measurements is doubtful especially during geomagnetic storms. Therefore, monitoring and forecasting these storms is imperative to mitigate their impacts.

We studied the Ionospheric variability during the four intense geomagnetic storms during the year 2015, a low solar activity period of the 24th solar cycle. The storms chronologically occurred on 17 March, 23 June, 07 October and 20 December. All the storms showed the value of Dst ≤ -100. The storm occurred on 17th of March 2015 was the most intense storm of the existing 24th solar cycle with the value of Dst -223nT. It is called the Saint Patrick's Day storm. For the present investigation, we considered three indices *viz.* Dst, F10.7cm solar flux and AE index. We also applied some statistical tools to study the variability of TEC during geomagnetic storms. We observed TEC variability at three international GNSS Service (IGS) stations at the low, mid and high latitude respectively, namely Mangilao, US (GUUG) at 13.44^{0}N & 144.80^0 E, Urumqi, China (URUM) at 43.82^{0}N & 87.60^0 E and Ny-Alesund, Norway (NYAL) at 78.92^{0}N & 11.86^0 E.

It was observed that out of these storms, the Saint Patrick's Day storm had the deepest impact on the Ionospheric TEC. It was also seen that during this storm statistical quantities (standard deviation and Average of TEC) also exhibited the highest numeric values. It was observed that low latitudes station showed a higher variation of TEC during the storm period. It was also seen that the Ionospheric TEC had shown synchronized variation with F10.7 solar flux and AE indices during geomagnetic storms.

Keywords: Geomagnetic storm, Dst index, AE index, F10.7cm.

Please cite this article as*: Parwani, Mahesh, Atulkar, Roshni, Ahmad, Rafi, Sharma, P.K and Purohit, P.K. (2019) Latitudinal ionospheric redistribution in northern hemisphere during geomagnetic storm. e-Journal Earth Science India, v. 12 (IV), pp. 191-202 https://doi.org/10.31870/ESI.12.4.2019.14*

INTRODUCTION

The sun continuously emits electromagnetic radiation like infrared, visible light and ultraviolet light due to the sustainable fusion process. The earth's external atmosphere is intensely affected by these electromagnetic radiations (Atulkar *et al.,* 2014). When the enormous cloud of plasma ejected from solar transient phenomena, interacts with the Earth's magnetic environment, they produce a geomagnetic storm (Gonzalez *et al.,* 1987; Sugiura *et al.,* 1960; Alabi *et al.,* 2015). Geomagnetic storms can be identified by the depression in H component of the geomagnetic field. It is derived by the Ring current encircling the Earth in a westward direction (Malvi *et al.,* 2016; Kamide, 1998; Daglis, 1999). In the upper atmosphere, a geomagnetic storm is a period of intense energy that is trapped in the magnetosphere and sustains from several hours to a few days. (Prolss, 2004; Rishbeth, 1998; Fuller-Rowell *et al.,* 1994).

The Magnetosphere is the region around the Earth where the magnetic field dominates. It provides protecting shield to the organism sustain on the Earth. The magnetosphere interacts with the solar wind and its accompanying field, this interaction gives the final shape to the magnetosphere. Whenever there is a very efficient exchange of energy transfers from the solar wind to the magnetosphere, it creates major disturbance into the magnetosphere and causes Geomagnetic storms. The most effective transferring of energy takes place when the solar wind magnetic field is directed southwards. *i.e.* opposite the direction of the geomagnetic field (Yurchyshyn *et al.,* 2010; Russell *et al.,* 1974; Tsurutani *et al.,* 1992).

The occurrence and intensity of a geomagnetic storm can be measured on the scale of Disturbance storm time (Dst). It is a measure of the variation in the horizontal component of the geomagnetic field at the equator due to change in the magnetospheric ring current. During quiet time its value is between +20 nT to -20 nT. A further decrease in the value of Dst indicates weaken the geomagnetic field or increased Ring current, which indicates the occurrence of a geomagnetic storm. The Ring current flows around the earth from the night time side to daytime side (westwards) and produces its own magnetic field like an electromagnet that is directed towards southwards (by the right-hand rule) *i.e.* against the Earth's dipole field. Thus, the increase in the ring current opposes the geomagnetic field and tries to compress it. This decline in the horizontal geomagnetic field is reported by negative values of Dst. According to the signature of Dst, Geomagnetic storm has three phases. The Initial phase, Main phase and Recovery phase. The initial phase shows the value of Dst from 20nT to 50nT. This phase lasts from a few minutes to some hours. It is also called sudden storm commencement (SSC). All storms do not have an initial phase, as not all the storms suffer a sudden increase in Dst. The main phase exhibits the value of Dst from -50nT to -600nT. It lasts from 2hrs to 8hrs; this phase gives rise to Ring current. The recovery phase as the name suggests, it takes the Dst back to quiet time values, it lasts form 8 hrs to 7 days. During this phase ring current or ion current gradually lost. On the scale of Dst the size of geomagnetic storms can also be classified into three categories; Moderate storm (-50nT to -100 nT), Intense storm (-100nT to -250 nT), Super storm (Dst more than -250nT).

An Ionospheric storm is almost always associated with geomagnetic storms. The intense current in magnetosphere significantly disturbs ionosphere (Fejer, 2007; Kikuchi, 2003; Rastogi, 1977). This disturbance in the ionosphere induces a severe increase or decrease in electron density in it. This ionization takes place when ionized particles ejected into the polar region or auroral zone. These particles ionize the D region and produce X-rays that further continue to ionize downwards (Akasofu *et al.,* 1965). The phenomenon is called Ionospheric storm. It has been fascinating researchers from the decades (Lin, 2005; Kane, 1973; Liu 2004; Fejer, 2002; Kutiev *et al.,* 2001).

This variation in ionosphere density changes the path of propagation of signals, therefore, creates errors in GPS positioning and navigation. The Ionospheric storms are categorized as Positive storm and Negative storm. The increase (decrease) in peak electron density and Total Electron Content (TEC) from its normal value is defined as Positive (Negative) Ionospheric storm (Parwani *et al.,*2019; Schunk *et al.,*1996; Danilov *et al.,*1985). This positive storm slow-down the speed of propagation of a signal, therefore causes time delay, range error and scintillation in communication and navigation (Balan *et al.,* 1990; Basu *et al.,* 2010; Basu, 2001; Pincheira, 2002; Purohit *et al.,* 2015; Christer *et al.,* 2014), whereas radio blackout is caused by Negative Ionospheric storms (Mendillo *et al.,* 2010; Rishbeth *et al.,*1991).

For the study of geomagnetic storms, we have considered two geomagnetic indices *viz.* Dst and AE indices and one solar activity index *i.e.* F10.7cm solar flux. Auroral Electrojet index (AE index) was developed in 1966. It is one of the most suitable indices for the study of geomagnetic storms. It is a measure of the total deviation of the horizontal component geomagnet (H) from its quiet time value, at an instant of time around the auroral oval. The index data are collected from the set of observatories forming form a necklace located underneath the auroral ovals in the northern hemisphere. This data is also applied for southern hemisphere due to lack of observatories in this region. The AE index is calculated by obtaining a one-minute resolution data from auroral observatories than five quiet days average value is subtracted from it.

F10.7cm solar flux is the most commonly used index for the study of the geomagnetic storm. It is used as a proxy for solar EUV flux due to their good correlation. The wavelength 10.7cm (frequency=2800MHz) is perfect for monitoring and measuring the solar activities, as it is sensitive for all physical solar conditions. It is a measurement of the strength of solar emission in a 100MHz wide band that is centered on 2800MHz (wavelength = 10.7cm) averaged over an hour. It may also be defined as the measurement of the whole emission on the wavelength 10.7cm from all the sources available at the solar disc, over 1hr period (sfu). $1sfu=10^{-22}Wm^{-2}Hz^{-1}$.

EVENT SELECTION CRITERION

To study the Ionospheric variability during geomagnetic storms, we had considered four geomagnetic storms during the year 2015; they chronologically occurred on 17 March, 23 June, 07 October, and 20 December. The storm occurred on 17^{th} of March 2015 was the strongest storm of the existing 24^{th} solar cycle with the value of Dst -223nT. It is also called the **Saint Patrick's Day storm**.

DATA SOURCES

We considered two types of data sets for the study:

(i) Ionospheric TEC data (Derived by GPS)
(ii) Geomagnetic Indices (Dst index and AE index) & Solar activity index (F 10.7 solar index)

Total Electron Content (TEC)

To investigate the latitudinal variation of ionospheric TEC, we had considered three IGS stations situated each at low, mid and high latitude. The selected stations with their codes and positioning details are shown in Table- 1.

The composition and behavior of the ionosphere can be described by various parameters derived from different instruments. The commonly used instruments are ionosonde and GPS. However, for the present study, we had downloaded the data of Ionospheric TEC for the three stations from the GPS network. The receivers of GPS are spread around the globe and the data is updated periodically. The TEC data is freely made available at the URL http://sopac.ucsd.edu/dataArchive/. This data is supplied in the internationally accepted data exchange format called RINEX (Receiver Independent Exchange Format). It is in the standard ASCII format (i.e. readable text). The raw data are further processed to convert into a suitable format, for this purpose, we used the software developed and freely made available by Dr. Gopi Krishna Seemala, Indian Institute of Geomagnetism (IIG), New Mumbai, India. This software is compatible to run on windows. It reads the RINEX format calculates receiver bias and reads satellite biases from the International GNSS Service (IGS) code files then produces data for analysis. The resolution of the obtained data is 30s.

Table- 1: Position of the chosen GPS stations.

S. No.	ID	location	Geo. latitude	Geo. longitude
1	GUUG	Mangilao, US	13.44^{0}N	144.80^0 E
2	URUM	Urumqi, China	43.82^{0}N	87.60^0 E
3	NYAL	Ny-Alesund, Norway	78.92^{0}N	11.86^0 E

Geomagnetic Indices (Dst index and AE index) & Solar activity index (F10.7 solar flux)

We considered 4 geomagnetic storms with a minimum value of Dst ≤ -100nT. We used three indices Dst, F10.7cm solar flux and AE index to study the effect the storms on ionospheric TEC. For the present study, we had downloaded five-day cycle of the index data from Space Physics Data Facility OMNI (http://omniweb.gsfc.nasa.gov/).

Table-2: Shows the intensity of the chosen geomagnetic storms.

Sr. No.	Date of the Event	Chronological order of the day	Minimum value of Dst
1	17 March 2015	76th day	-223nT
2	23 June 2015	174th day	-204nT
3	07 October 2015	280th day	-124nT
4	20 December 2015	354th day	-155nT

RESULTS AND DISCUSSION

The upset geomagnetic conditions cast a deep impact on the ionosphere. To study the variability of Ionospheric TEC at three chosen GPS stations, during disturbed geomagnetic conditions. We had investigated the geomagnetic storms. All the four events are discussed below in chronological order.

Event 1: 17 March 2015

One of the most intense geomagnetic storms of the 24th solar cycle was recognized on 17 March 2015. From Fig. 1, it was seen that the Ionospheric TEC over the low and the high latitude stations obtain the peak of their cycle on 17 March. It was also observed that during storm periods TEC over the low latitude station obtained the highest peak and over the mid latitude station obtained the lowest peak. It indicates the low latitude region experienced the maximum impact of the storm, whereas the mid latitude station experienced the least disturbance during the main phase of the storm.

The Fig. 1 also shows that during the storm period the Ionospheric TEC exhibited synchronized variation with F10.7 solar flux and AE indices. It was also noticed that ionospheric TEC at low latitude station seems to be more responsive to the indices, therefore showed better synchronization with these indices. It was also seen that during the main phase of the storm, when Dst moved towards its negative peak (-223nT), the values of ionospheric TEC for all three stations moved towards their positive peaks. In other the words, the TEC over the three latitudes showed negative synchronization with Dst index. It was also noticed that during the recovery phase all the parameter returns to their quiet time values.

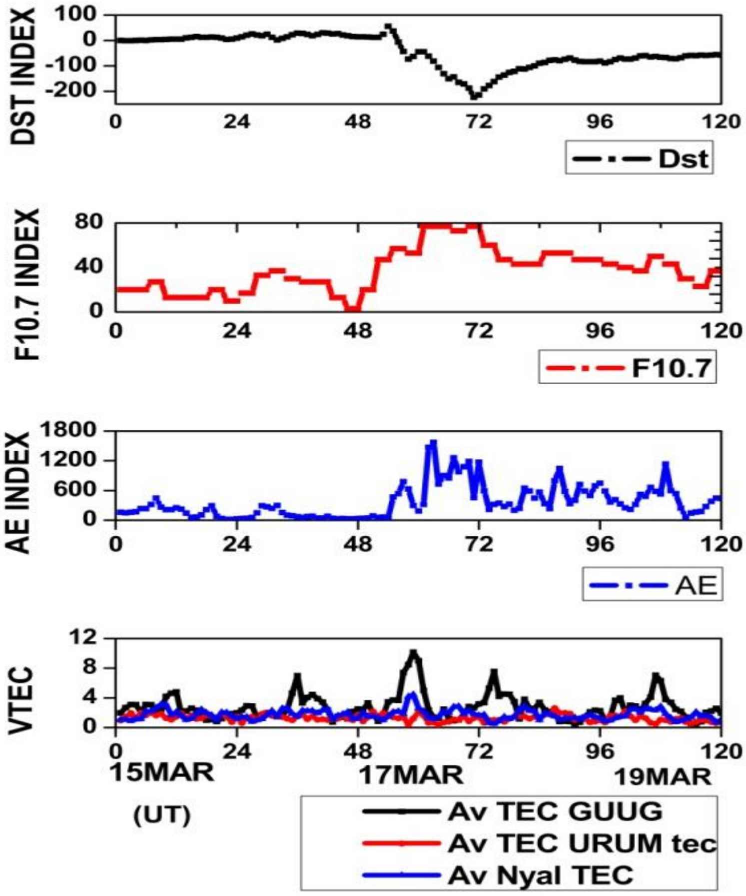

Fig. 1: Day to day variations of TEC (at low, mid & high latitude) along with Dst, AE and F10.7cm indices from 15 to 19 March 20015.

Event 2: 23 June 2015

Another intense storm occurred on 23 June 2015, with the minimum value of Dst-204nT. From Fig. 2, it was observed that the Total Electron Content (TEC) at low, mid and high latitude stations obtained the peak of their cycle during the main phase. It was seen that during the storm period the low latitude station obtained the highest peak of TEC, that indicates that the low latitude region bears the deeper impact of the storm than that of the other two latitudes. It was also seen that the high latitude station experiences the least disturbance in Ionospheric TEC during the main phase of the storm.

Fig. 2 also shows that during the storm period the Ionospheric TEC displayed synchronized variation with F10.7 solar flux and AE indices. Moreover, it was seen that low latitude Ionospheric TEC showed better synchronization with the indices. It was also seen that during the main phase of the storm, when Dst dipped to its negative peak, the values of ionospheric TEC over all three stations hiked to their positive peaks. In other words, TEC showed reverse synchronization with Dst. It was also noticed that during the recovery phase all the parameter returns to their quiet time values

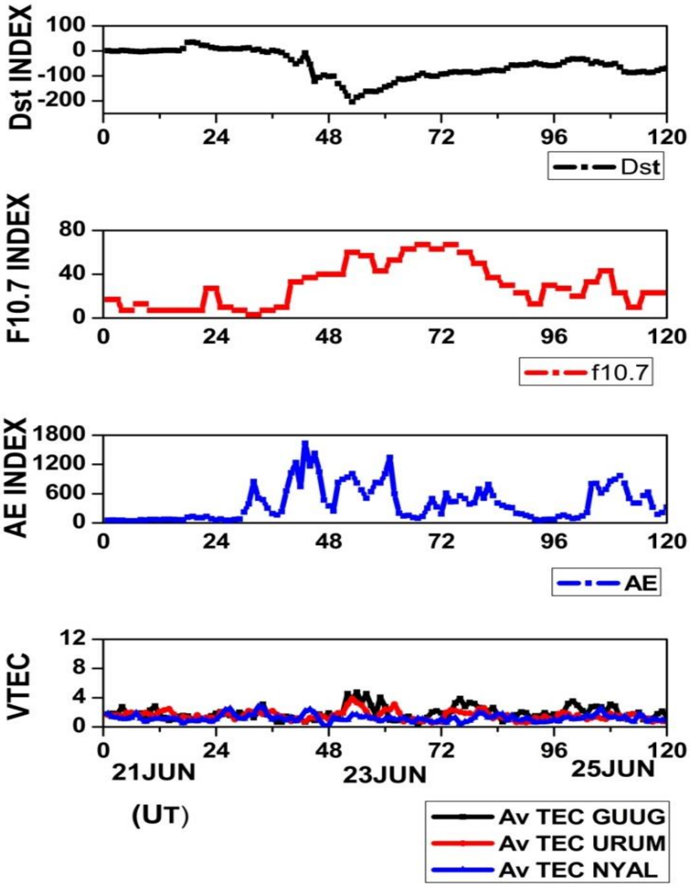

Fig. 2: Day to day variation of TEC (at low, mid & high latitude) along with Dst, AE and F10.7cm indices from 21 to 25 June 2015

Event 3: 07 October 2015

Another intense geomagnetic storm (Dst at -124nT) occurred on 07 October 2015. From figure 3, it was seen that the Ionospheric TEC over low, mid and high latitude stations obtained the peak of their cycle during the main phase of the storm. Moreover, it was also seen that the low latitudinal station obtained higher peak than that of the mid or high latitude stations, that indicates that the low latitude region suffered maximum disturbance in TEC during the main phase of the storm.

Fig. 3 shows that the Ionospheric TEC had synchronized variation with F10.7 and AE indices. It was also observed that low latitude Ionospheric TEC showed better synchronization with these indices. It was also seen that when Dst was dipped to its negative peak, then the values of ionospheric TEC for all three stations approached towards their positive peaks. In other words, TEC showed reverse synchronization with Dst. during the period. It was also noticed that during storm time, ionospheric TEC showed the maximum variation over the low latitude station and minimum variation over mid latitude station. Further, it was noticed that during the recovery phase all the parameter returns to their quiet time values.

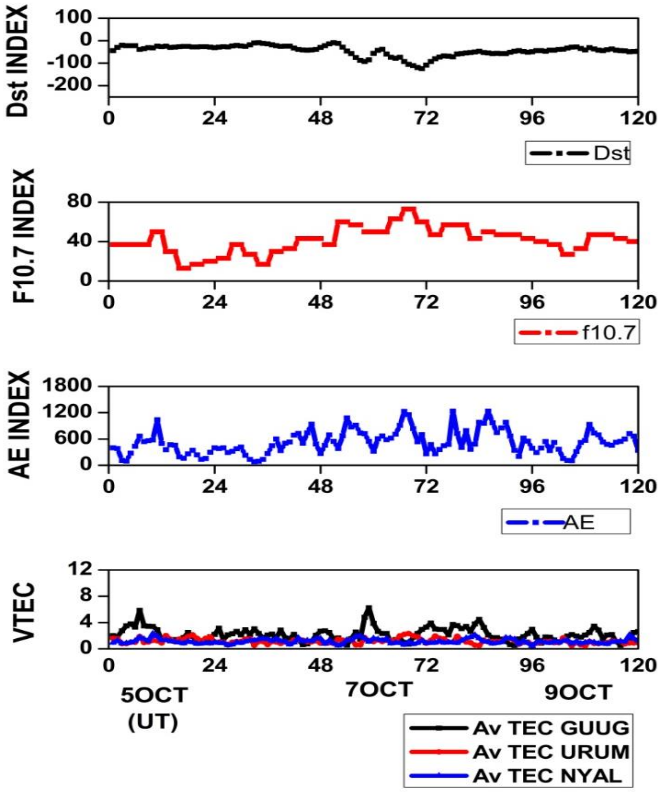

Fig. 3: Day to day variation of TEC (at low, mid & high latitude) along with Dst, AE and F10.7cm indices, from 05 to 09 Oct 2015.

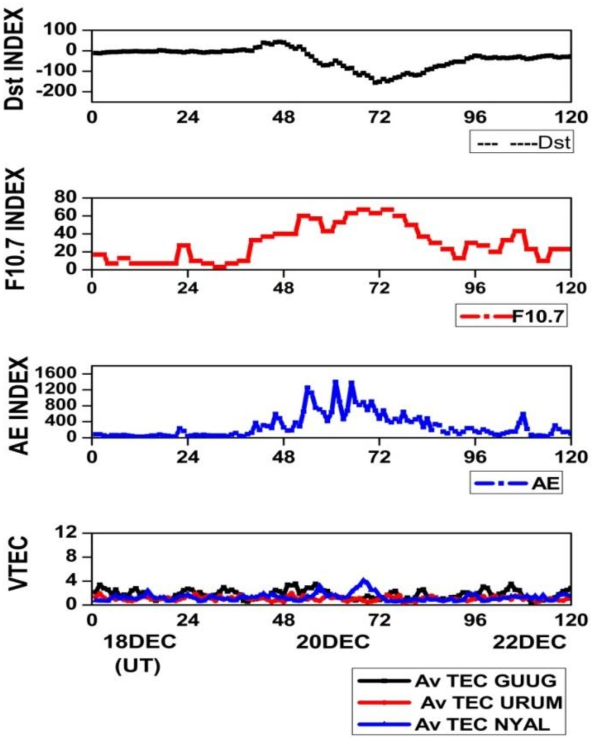

Fig. 4: Day to day variation of TEC (at low, mid & high latitude) along with Dst, AE and F10.7cm indices from 18 to 22 Dec 2015.

Event 4: 20 December 2015

The intense geomagnetic storm with Dst -155nT occurred on 20 December 2015. From the figure, it was seen that Ionospheric TEC over low and high latitude stations moved towards the peak of their cycle during the main phase of the storm. It was also seen that the mid latitude station experienced less disturbance in Ionospheric TEC than that of the low and mid latitude.

The figure also shows that the Ionospheric TEC exhibited synchronized variation with F10.7 and AE indices. Moreover, high latitude Ionospheric TEC was more responsive, therefore, showed better synchronization. It was also seen that TEC showed reverse synchronization with Dst. during the main phase of the storm. Further, it was noticed that during the recovery phase all the parameter returns to their quiet time values.

Statistical Characteristics of Ionospheric Variation

We used two statistical tools *viz.* Standard Deviation (STD) and Average (Av) to study the latitudinal variability of TEC during the geomagnetic storms. For this purpose, we had calculated hourly Average (Av) and Standard Deviation (STD) of ionospheric TEC for the storm period (*i.e.* 5 storm days). All the events are discussed below in chronological order.

Event 1: 17 March 2015

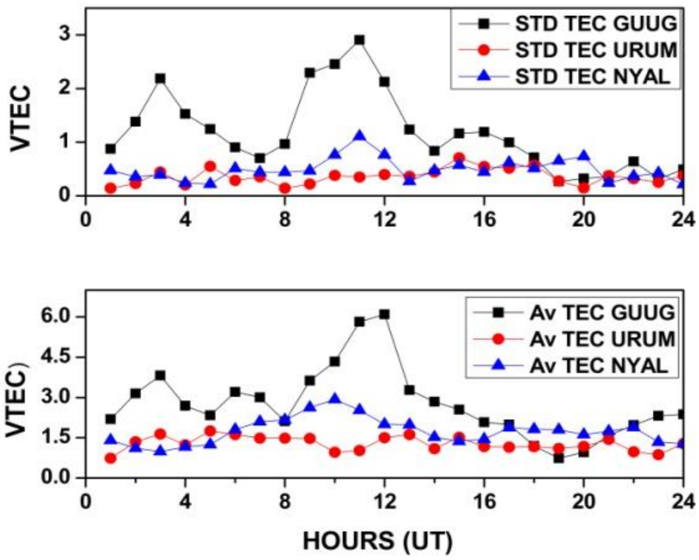

Fig. 5: Hourly Standard Deviation and Average of TEC at low, mid and high latitude stations from 15 to 19 March 2019.

Fig. 5 shows standard deviation and Average of hourly Ionospheric TEC from 15 to 19 March at low, mid and high latitude stations. From the figure, it was seen that TEC over low latitude station showed the highest values of standard deviation and hourly Average than that of mid and high latitude stations. It was also observed that mid latitude station shows the least value of Standard Deviation and Average of Ionospheric TEC than that of the low and high latitude stations.

Event 2: 23 June 2015

Fig.6 shows the hourly standard deviation and Average of Ionospheric TEC at low, mid and high latitude stations. From the figure, it is seen that TEC over low latitude station showed the higher values of standard deviation as well as hourly Average than that of the mid and high latitude regions. In other words, low latitude station sustained the maximum effect during the geomagnetic storm. It was also seen that both the statistical quantities exhibited higher values during the first half of the day.

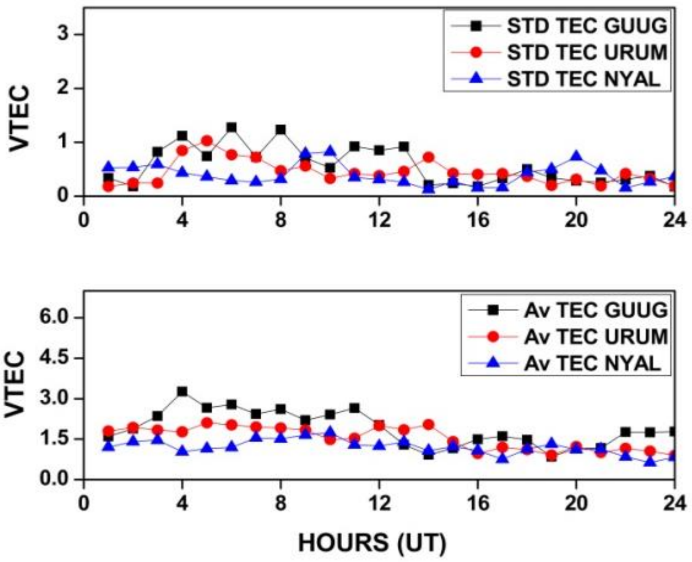

Fig. 6: Hourly Standard Deviation and Average of ionospheric TEC at low, mid and high latitude stations from 21 to 26 June 2019.

Event 3: 07 October 2015

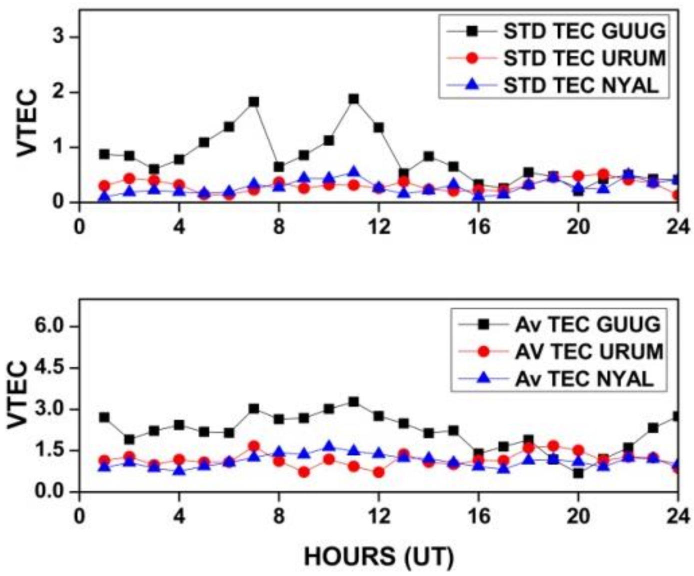

Fig. 7: Hourly Standard Deviation and Average of ionospheric TEC at low mid and high latitude stations from 05 to 09 Oct 2019

The Fig. 7 shows the hourly standard deviation and the Average of Ionospheric TEC at low, mid and high latitude stations. From the figure, it is seen that TEC over low latitude station showed the highest values of standard deviation as well as hourly Average than that of the mid and low latitude regions. It was also seen that both the statistical quantities showed higher values during the first half of the day, during the storm period.

Event 4: 20 December 2015

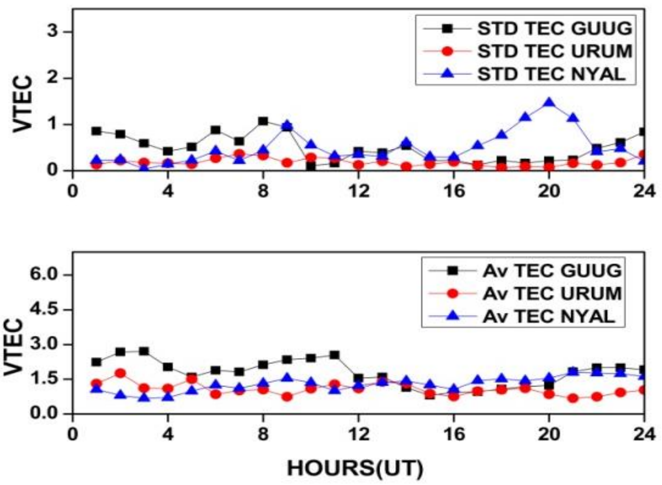

Fig. 8. Hourly Standard Deviation and Average of TEC data from 18 to 22 Dec 2015, at low mid and high latitude stations.

Fig.8 shows the hourly standard deviation and the Average of Ionospheric TEC at low, mid and high latitude stations. It was also seen that both the statistical quantities, *i.e.* Standard Deviation and Average of TEC showed higher values during the first half of the day, during the storm period. It was also observed that TEC over low latitude station showed the highest values of standard deviation and hourly Average than that of the mid and high latitudes. It was also observed that mid latitude station showed less value of Standard Deviation and Average of Ionospheric TEC during the storm period.

CONCLUSION

(i) It was observed that out of the four storms of the year 2015, Saint Patrick's Day storm was the strongest one, which induced maximum variation in the Ionospheric TEC and produced highest peaks in the TEC graph. It indicates that during the storm period the TEC variation correlated with the intensity of the storm.

(ii) It was observed that during geomagnetic storms, low latitudes station showed a higher variation of TEC than that of mid and high latitude stations.

(iii) It was also observed that during geomagnetic storms, the mid latitude region exhibits lowest variation ionospheric TEC than that of low and high latitude regions, in other words, that during geomagnetic storms mid latitude is least affected region.

(iv) It was seen that the Ionospheric TEC showed synchronized variation with F10.7 and AE indices. Moreover, low latitude Ionospheric TEC seems to be better responsive to the indices.

(v) It was also observed that statistical tools viz. Standard Deviation and Average of Ionospheric TEC obtain higher numeric values during **Saint Patrick's Day storm** (most intense storm of the 24th solar cycle) than that of any other storm during 2015.

(vi) It was also seen that ionospheric TEC over low latitude station registered the highest peak of Standard Deviation and Average ionospheric TEC than that of mid and high latitude stations, during the storms occurred in s2015.

(vii) It was also observed that during all the storms, Standard Deviation and Average of Ionospheric TEC shows higher values during the first half of the day during the storm period.

Acknowledgements: The authors are thankful to various online data servers sites like Scripps Orbit and Permanent Array Center SOPAC (URL http://sopac.ucsd.edu/dataArchive/.), Space Physics Data Facility OMNI (http://omniweb.gsfc.nasa.gov/), http://irimodel.gov/, and Dr. Gopi Krishna Seemala, for freely distributing the software to process raw TEC data.

REFERENCES

Akasofu, S. I., Chapman, S. and Meng, C. I. (1965) The Polar electrojet. Atmosph. Terr. Phys., v. 27, pp. 1275-1305.

Alabi, O. O., Adebesin, B. O., Ikubanni, S. O. and Sedara, S.O. (2015) Comparative analysis into the geomagnetic indices (ap, ae, dst, bz) during disturbed period and quiet conditions of solar maximum year (2001). Innovative Space of Scientific Research Journals, v.17(1), pp. 155-163.

Atulkar, Roshni, Bhardwaj, Shivangi, Khatarkar, Prakash, Bhawre, Purushottam and Purohit, P. K. (2014) Geomagnetic disturbances and its impact on ionospheric critical frequency (foF2) at high, mid and low latitude region. American Journal of Astronomy and Astrophysics, v. 2(6), pp. 61-65. doi: 10.11648/j.ajaa.20140206.11

Balan, N. and Rao, P. B. (1990) Dependence of ionospheric response on the local time of sudden commencement and intensity of storms. J. Atm. Terr. Phys., v. 52, pp. 269–275.

Basu, S. (2001) Response of the equatorial ionosphere in the South Atlantic region to the great magnetic storm of July 15, 2000. Geophys. Res. Lett., v. 28, pp. 3577–3580.

Basu, S., MacKenzie, E., Bridgwood, C., Valladares, C.E., Groves, K.M. and Carrano, C. (2010) Specification of the occurrence of equatorial ionospheric scintillations during the main phase of large magnetic storms within solar cycle 23. Radio Sci., v. 45, pp. RS5009. doi:10.1029/2009RS004343

Christer van der, Meeren, Kjellmar, Oksavik, Dag Lorentzen, JøranIdar, Moen and Vincenzo, Romano (2014) GPS scintillation and irregularities at the front of an ionization tongue in the nightside polar ionosphere. J. Geophys. Res. Space Physics, v. 119, pp. 8624–8636. doi:10.1002/2014JA020114.

Daglis, I. A. (1999) The terrestrial ring current: Origin, formation, and decay. Rev. Geophys., v.37, pp. 407– 438.

Danilov, A. D. and Morozova L. D. (1985) Ionospheric storms in the F2 region: Morphology and physics (Review). Geomagn. Aeron., v. 25, pp. 593–605.

Fejer, B. G. (2002) Low latitude ionospheric electrodynamics. J. Atm. Terr. Phys., v. 64, pp. 1401–1408.

Fejer, B. G. (2007) Equatorial ionospheric electric fields during the November 2004 magnetic storm. J. Geophys. Res., v. 112, pp. A10304. doi:10.1029/2007JA012376.

Fuller-Rowell, T.J., Codrescu, M.V., Moffett, R.J. and Quegan, S. (1994) Response of the thermosphere and ionosphere to geomagnetic storms. J. Geophys. Res., v. 99, pp. 3893–3914. doi:10.029/93JA02015.

Gonzalez, W. D. and Tsurutani, B. T. (1987) Criteria of interplanetary parameters causing intense magnetic storms (Dst< 100 nT). Planet Space Sci., v.35, pp. 1101–1109.

Kamide, Y. (1998) Current understanding of magnetic storms' Storm-substorm relationships. J. Geophys. Res., v.103, pp. 17,705– 17,728.

Kikuchi, T. (2003) Equatorial counter electrojets during a substorm. J. Geophys. Res., v. 108 (A11) pp. 1406. doi:10.1029/2003JA009915.

Kane, R. P. (1973) Global evolution of F2-region storm. J. Atmos. & Solar Terres. Phys., v. 35, pp. 1953–1966.

Kutiev, I. and Muhtarov, P. (2001) Modeling of mid-latitude F region response to geomagnetic activity. J. Geophys. Res., v. 106, pp. (A8) 15501–15509.

Lin, C. H. (2005) Large-scale variations of the low-latitude ionosphere during the October–November 2003 superstorm: Observational results. J. Geophys. Res., v. 110, pp. (A09S28) doi:10.1029/2004JA010900.

Liu, L. (2004). The low latitude ionospheric effects of the April 2000 magnetic storm near. Earth Planet Space, v.56, pp. 607– 612.

Malvi, Bhupendra, Srivastav, Prateek S., Azad, A. Mansoori, Atulkar, Roshni, Bhardwaj, Shivangi and Purohit, P. K. (2016) Morphological investigation of disturbed Ionosphere during Intense Geomagnetic Storms. XXVII IUPAP Conference on Computational Physics (CCP2015) IOP Publishing, Journal of Physics: Conference Series, v. 759, pp. 012067, doi:10.1088/1742-6596/759/1/012067.

Mendillo, M. and Narvaez, C. (2010) Ionospheric storms at geophysically equivalent sites-Part. Ann. Geophys., v.28, pp. 1449–1462.

Parwani, Mahesh, Atulkar, Roshni, Mukherjee, Shweta and Purohit, P. K. (2019) Latitudinal variation of ionospheric TEC at Northern Hemispheric region. Russian Journal of Earth Sciences. v. 19, pp. ES1003, doi:10.2205/2018ES000644.

Pincheira, X. T. (2002) An investigation of ionospheric responses and disturbance thermospheric winds, during magnetic storms over South America sector. J. Geophys. Res., v. 107, pp. (A11) 1379. doi:10.1029/2001JA000263.

Prölss, G.W. (2004) Space weather effects in the upper atmosphere: low and middle Latitudes. Space Weather. pp 193-214 Part III Models of Space Weather.

Purohit, P. K., Mansoori, Azad A., Khan, Parvaiz A., Atulkar, Roshni, Bhawre, Purushottam, Tripathi, Sharad C., Khatarkar, Prakash, Bhardwaj, Shivangi, Aslam, A. M., Waheed, Malik A. and Gwal A. K. (2015) Evaluation of geomagnetic storm effects on the GPS derived Total Electron Content (TEC). XXVI IUPAP Conference on Computational Physics (CCP2014), IOP Publishing Journal of Physics: Conference Series 640 (2015) 012072. doi:10.1088/1742-6596/640/1/012072

Rastogi, R. G. (1977) Geomagnetic storms and electric fields in the equatorial ionosphere. Nature, v.268, pp. 422–424.

Rishbeth, H. (1991) F-region storms and thermospheric dynamics. Journal of Geomagnetism and Geoelectricity, v.43, pp. 513–524.

Rishbeth, H. (1998). How the thermospheric circulation affects the ionospheric F2-layer.J. Atmos. Terr. Phys., v. 60, pp. 1385–1402.

Russell, C. T., McPherron, R. L., and Burton, R. K. (1974) On the cause of geomagnetic storms. J. Geophys. Res., v. 79(7), pp. 1105–1109.

Schunk, R. W. and Sojka, J. J. (1996) Ionosphere-thermosphere space weather issues. J. Atmos. Sol. Terr. Phys., v. 58, pp. 1527–1574. doi:10.1016/0021-9169(96)00029-3.

Sugiura, M. and Chapman, S. (1960) The average morphology of geomagnetic storms with sudden comencement, Abandl. Akad. Wiss. Gottingen Math. Phys.K1 (4).

Tsurutani, B. T., Gonzalez, W. D., Tang, F. and Lee, Y. T. (1992) Great magnetic storms. Geophys. Res. Lett., v. 19(1), pp. 73 – 76.

Yurchyshyn, Vasyl and Tripathi, Durgesh (2010) Relationship between earth-directed solar eruptions and magnetic clouds at 1au: a brief review. Advances in Geosciences, pp. 51-70. http://dx.doi.org/10.1142/9789812838209_0004.

(Received: 07.08.2019; Accepted: 22.10.2019)